Dipole-Bound Anion of the HNNH₃ Isomer of Hydrazine. An Ab Initio Study

Piotr Skurski

Department of Chemistry, University of Utah, Salt Lake City, Utah 84112, and Department of Chemistry, University of Gdańsk, 80-952 Gdansk, Poland

Maciej Gutowski

Materials and Chemical Sciences, Pacific Northwest National Laboratory, Richland, Washington 99352

Jack Simons*

Department of Chemistry, University of Utah, Salt Lake City, Utah 84112

The possibility of electron binding to the $HNNH_3$ and H_2NNH_2 tautomers of hydrazine was studied at the coupled cluster level of theory with single, double, and noniterative triple excitations. The $HNNH_3$ tautomer, with a dipole moment of 5.4 D, binds an electron by 1076 cm^{-1} whereas the H_2NNH_2 tautomer forms neither a dipole- nor valence-bound anionic state. It is suggested that the $HNNH_3$ tautomer, which is kinetically stable but thermodynamically unstable relative to H_2NNH_2, may be formed by photodetachment from the $N_2H_4^-$ species examined in this work.

1. Introduction

1.1. Hydrazine and Its Tautomer. The nitrogen atom is present in a large number of functional groups contained in many organic and inorganic compounds. There are, however, comparatively few compounds containing the singly bonded >N–N< fragment, because such systems are destabilized by the repulsion of nitrogens' lone electron pairs. The parent compound, hydrazine (H_2NNH_2), is kinetically stable, but thermodynamically unstable.[1] It is one of the simplest nitrogen compounds and an important rocket fuel; thus it has been well characterized experimentally[2–10] and theoretically.[11–20]

The C_2 symmetry gauche conformer of hydrazine (see Figure 1, **III**) is known experimentally and theoretically to be the most stable structure. Rotation around the N–N bond leads to the less stable staggered (anti) C_{2h} conformer and an eclipsed (syn) structure. The latter conformer corresponds to a transition state on the potential energy surface, whereas the former is a local minimum.

The second tautomer of hydrazine (iminoammonium, $HNNH_3$ (see Figure 1, **I**)), has been studied theoretically by Pople et al.[21] They considered **I** as the ammonia–nitrene complex created via a 1,2-hydrogen shift in H_2NNH_2 and found that **I** is less stable than **III** by 49.8 kcal/mol at the MP4/6-31G* level. They also found that the barrier for the **I** ↔ **III** tautomerization, via a C_1 symmetry transition state **II** (see Figure 1), amounts to 19 kcal/mol at the MP4/6-31G* level. The $HNNH_3$ tautomer has also been studied by Ding and Zhang at the MP2/6-31G**// SCF/6-31G** level.[22]

Past studies on the ionic species have been devoted to the $N_2H_4^+$ cation and its various structures.[18,23] As far as the negative ions are considered, an experimental study of the dissociative electron attachment to hydrazine was performed and formation of NH_2^- by the attachment of an electron to H_2NNH_2 was reported.[24] To the best of our knowledge, the possibility of formation of stable $N_2H_4^-$ anions has, to date,
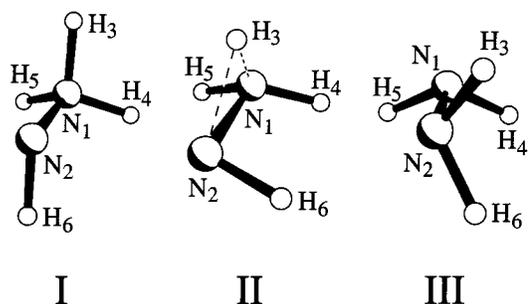
Figure 1. Geometries of $HNNH_3$ (**I**) and the transition state (**II**) for the tautomerization leading to the gauche tautomer (**III**). The structures of the $(HNNH_3)^-$ and anionic transition state are visually indistinguishable from their neutral counterparts.

been investigated neither experimentally nor theoretically, even though the significant SCF dipole moment of 5.5 D for **I**[22] leaves no doubt[25] that a dipole-bound anion of this isomer may be formed.

We have recently found that the phosphorus analogue of hydrazine, i.e., P_2H_4, does not form a bound *valence* anionic state.[26] However, the $HPPH_3$ isomer, with an SCF dipole moment of 4.1 D, binds an electron by 333 cm^{-1} with electron correlation contributing 82% of the electronic stability. In the current study we explore electron binding by the **I** and **III** isomers of hydrazine. Both valence and dipole-bound anions are considered, and electron correlation effects are included at the coupled cluster level of theory with single, double, and noniterative triple excitations.

1.2. Dipole-Bound Anions. The binding of electrons to polar molecules has been addressed in many theoretical[26–42] and experimental[43–47] studies. It has been shown that, within the Born–Oppenheimer (BO) approximation, a dipole moment greater than 1.625 D possesses an infinite number of bound anionic states,[47–51] although the more practical critical value

required to experimentally observe a dipole-bound anion was found to be slightly larger, about 2.5 D.[43,52]

Jordan and Luken demonstrated that the loosely bound electron in a dipole-bound state occupies a diffuse orbital localized mainly on the positive side of the dipole.[28] This finding was confirmed by many recent studies. The role of non-BO coupling has been studied by Garrett, who concluded that such couplings are negligible for dipole-bound states with electron binding energies (E_{bind}'s) much larger than the molecular rotational constants.[53]

The simplest theoretical approach to estimate E_{bind} is based on Koopmans' theorem.[54] The KT binding energy (E_{bind}^{KT}) is the negative of the energy of the relevant unfilled orbital obtained from a Hartree−Fock self-consistent field (SCF) calculation on the *neutral* molecule. The orbital relaxation effects, which are neglected in the KT approximation, have been found to be quite small for a variety of dipole-bound anionic states.[26,29−37] In contrast, the role of electron correlation has proven to be very significant. In fact, in many cases the electron binding energy of the dipole-bound anion has been dominated by the contribution from electron correlation.[26,31−38] The very recent studies on dipole-bound anions of hydrogen-bonded clusters[39−41] and CH_3NO_2[42] yielded similar conclusions.

Based on the experience mentioned above, we earlier concluded that the electron correlation contributions to E_{bind} encompass (i) a stabilizing dynamical correlation between the loosely bound electron and the electrons of the neutral molecule and (ii) an improved description of the charge distribution (and hence the dipole moment) of the neutral. Furthermore, we found that effects beyond the second-order Møller−Plesset (MP2) level can contribute substantially to the stability of dipole-bound anionic states and solvated electrons.[26,31−37]

Probably the most spectacular cases in which correlation is important involve the dipole-bound anions of water−ammonia and HPPH$_3$, where we found that electron correlation contributes respectively 77 and 82% to the electron binding energy.[26,36] In the present paper, we explore the role of electron correlation effects in electron binding to HNNH$_3$.

2. Methods

2.1. Decomposition of E_{bind} into Various Physical Components. In this work we present the results of highly correlated ab initio calculations for the anion of N_2H_4. We studied the potential energy surfaces of the neutral and anionic system at the MP2 level of theory and we calculated the values of E_{bind} using a supermolecular approach (i.e., by subtracting the energies of the anion from those of the neutral). This approach requires the use of size-extensive methods, so we have employed Møller−Plesset perturbation theory up to fourth order as well as the coupled-cluster method with single, double, and noniterative triple excitations (CCSD(T)).[55,56] In addition, E_{bind} was analyzed within a perturbation framework designed for dipole-bound anions and solvated electrons.[34]

Orbital relaxation and electron correlation corrections, which are neglected when E_{bind} is calculated at the KT level of theory, were taken into account by performing self-consistent field (SCF) and correlated CCSD(T) electronic structure calculations for the neutral and the anion.

The polarization of the neutral host by the excess electron and the effect of back-polarization are taken into account when the SCF calculation is performed for the anion, and the accompanying induction effects are given by

$$\Delta E_{bind}^{SCF-ind} = E_{bind}^{SCF} - E_{bind}^{KT} \tag{1}$$
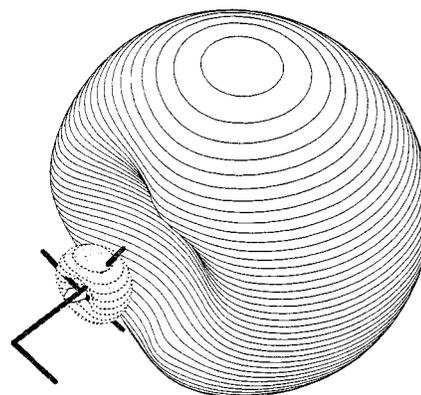
Figure 2. Singly occupied molecular orbital (SOMO) of the (HNNH$_3$)$^-$ (plotted with a 0.012 contour spacing).

where

$$E_{bind}^{SCF} = E_N^{SCF} - E_A^{SCF} \tag{2}$$

and E_N^{SCF} and E_A^{SCF} are the SCF energies of the neutral (N) and the anion (A), respectively.

The dispersion interaction between the loosely bound electron (lbe) and the neutral host was extracted from the MP2 contribution to E_{bind}.[34] The dispersion term is a second-order correction with respect to the fluctuation-interaction operator,[34] and it is approximated here by $\Delta E_{bind}^{MP2-disp}$, which takes into account proper permutational symmetry for all electrons in the anion

$$\epsilon_{disp}^{(02)} \approx -\Delta E_{bind}^{MP2-disp} = \sum_{a \in N} \sum_{r<s} \frac{|\langle \phi_a \phi_{lbe} || \phi_r \phi_s \rangle|^2}{e_a + e_{lbe} - e_r - e_s} \tag{3}$$

where ϕ_a and ϕ_{lbe} are spin orbitals occupied in the UHF wave function, ϕ_r and ϕ_s are unoccupied orbitals, and e's are the corresponding orbital energies. The total MP2 contribution to E_{bind} defined as

$$\Delta E_{bind}^{MP2} = E_{bind}^{MP2} - E_{bind}^{SCF} \tag{4}$$

is naturally split into the dispersion and nondispersion terms

$$\Delta E_{bind}^{MP2} = \Delta E_{bind}^{MP2-disp} + \Delta E_{bind}^{MP2-no-disp} \tag{5}$$

with the latter being dominated by the correlation correction to the static Coulomb interaction between the extra electron and the charge distribution of N.[34]

The higher-order MP contributions to E_{bind} are defined as

$$\Delta E_{bind}^{MPn} = E_{bind}^{MPn} - E_{bind}^{MP(n-1)} \qquad n = 3, 4 \tag{6}$$

Finally, the contributions beyond the fourth order are estimated by subtracting the MP4 results from those obtained at the coupled-cluster level

$$\Delta E_{bind}^{CC} = E_{bind}^{CC} - E_{bind}^{MP4} \tag{7}$$

In particular, the DQ, SDQ, and SDTQ MP4 energies are subtracted from the D, SD, and SD(T) coupled cluster binding energies, respectively.[55]

2.2. Computational Details. The diffuse character of the orbital describing the loosely bound electron (see Figure 2) necessitates the use of extra diffuse basis functions having very low exponents.[28] In addition, the basis set chosen to describe

TABLE 1: Geometries and Harmonic Vibrational Frequencies for the Neutral and Dipole-Bound Anionic States of HNNH$_3$ at the Stationary Points (minima)^a (Frequencies in cm^{-1}, Distances (r) in Å, Valence (α) and Dihedral (δ) Angles in Degrees, Dipole Moment μ of the Neutral Dimer in D, Zero-Point Vibrational Energies (E_0^{vib}) in kcal/mol)^b

system	geometry	μ_{neutral} SCF	μ_{neutral} QCISD	frequencies	E_0^{vib}
HNNH$_3$	$r(N_1N_2) = 1.459$, $r(N_1H_3) = 1.023$ $r(N_1H_4) = 1.032$, $r(N_2H_6) = 1.030$ $\alpha(H_3N_1N_2) = 105.19$, $\alpha(H_4N_1N_2) = 115.57$ $\alpha(H_3N_1H_4) = 106.32$, $\alpha(N_1N_2H_6) = 102.23$ $\delta(H_3N_1H_4N_2) = 116.27$	5.47	5.40^c	$\omega_1(a'') = 361$, $\omega_2(a') = 879$ $\omega_3(a') = 1024$, $\omega_4(a'') = 1061$ $\omega_5(a') = 1449$, $\omega_6(a') = 1477$ $\omega_7(a'') = 1643$, $\omega_8(a') = 1661$ $\omega_9(a') = 3300$, $\omega_{10}(a'') = 3355$ $\omega_{11}(a') = 3430$, $\omega_{12}(a') = 3539$	33.14
HNNH$_3^-$	$r(N_1N_2) = 1.460$, $r(N_1H_3) = 1.024$ $r(N_1H_4) = 1.033$, $r(N_2H_6) = 1.031$ $\alpha(H_3N_1N_2) = 106.30$, $\alpha(H_4N_1N_2) = 115.86$ $\alpha(H_3N_1H_4) = 105.79$, $\alpha(N_1N_2H_6) = 102.03$ $\delta(H_3N_1H_4N_2) = 117.46$	5.50	5.42^d	$\omega_1(a'') = 341$, $\omega_2(a') = 902$ $\omega_3(a') = 1025$, $\omega_4(a'') = 1066$ $\omega_5(a') = 1452$, $\omega_6(a') = 1473$ $\omega_7(a'') = 1639$, $\omega_8(a') = 1653$ $\omega_9(a') = 3290$, $\omega_{10}(a'') = 3357$ $\omega_{11}(a') = 3422$, $\omega_{12}(a') = 3519$	33.08

^{a} For the numbering of atoms, see Figure 1 (structure **I**). ^{b} MP2 results obtained with the aug-cc-pVDZ basis set supplemented with the 6s6p4d diffuse set. ^{c} MP2, MP3, and MP4(SDQ) values of dipole moment: 5.46, 5.45, and 5.41 D, respectively. ^{d} MP2, MP3, and MP4(SDQ) values of dipole moment: 5.48, 5.47 and 5.43 D, respectively.

the neutral molecular host should be flexible enough to (i) accurately describe the static charge distribution of the neutral and (ii) allow for polarization and dispersion stabilization of the anion upon electron attachment. The majority of our calculations were performed with aug-cc-pVDZ basis sets[57] supplemented with diffuse s, p, d, and sometimes f functions centered on the atom labeled N$_1$ in Figure 1 (since this is the centroid of the positive end of the dipole). The extra diffuse s, p, and d functions do not share exponent values, but the exponents of the f functions were the same as those used for the d functions. The results presented below justify our basis set selection.

We explored the dependence of E_{bind} on the choice of the extra diffuse functions. These tests were performed with the aug-cc-pVDZ core basis set with only the extra diffuse functions being varied. We used even-tempered six-term s, six-term p, and four-term d basis sets. The geometric progression ratio was equal to 3.2,[58] and for every symmetry we started to build up the exponents of the extra diffuse functions from the lowest exponent of the same symmetry included in aug-cc-pVDZ basis set designed for nitrogen. As a consequence, we achieved the lowest exponents of 5.7034×10^{-5}, 5.2257×10^{-5}, and 2.1935×10^{-3} a.u. for the s, p, and d symmetries, respectively.

Next, we determined that the MP2 electron binding energy increases by only 2 cm^{-1} after inclusion of a four-term set of diffuse f functions. We also explored the dependence of E_{bind} on the *core* basis set chosen to describe the neutral molecular host. The MP2 value of E_{bind} obtained with Dunning's aug-cc-pVTZ basis set,[57] with the six-term s, six-term p, and four-term d diffuse set fixed, differs by less than 3 cm^{-1} from the results obtained using the aug-cc-pVDZ basis instead. We therefore believe that our MP2 electron binding energies obtained with the aug-cc-pVDZ basis set supplemented with the six-term diffuse s and p, and four-term diffuse d functions underestimate the correct binding energy by less than 5% due to basis set incompleteness.

Therefore, our final basis set was selected to be the aug-cc-pVDZ basis supplemented with the 6s6p4d diffuse set for the optimization of geometries, for calculating frequencies, and for evaluating the electron binding energies.

In computing correlation energies, all orbitals except the 1s orbitals of nitrogen were included, and all results reported in this study were obtained with the Gaussian 94 program.[59] Finally, to avoid erroneous results caused by using Gaussian 94's (default) direct SCF module with the large s, p, d, and f

sets of diffuse functions, we performed conventional SCF calculations. Moreover, the two-electron integrals were evaluated (without prescreening) to a tolerance of 10^{-20} au in the single-point calculations.

3. Results

We did not find a valence-bound anionic state for either the gauche or staggered conformations of H$_2$NNH$_2$ or for HNNH$_3$. The dipole moment of 2.0 D for the gauche structure **III** is too small to substantially bind an excess electron. This finding was not surprising in light of the fact that the electron binding energy for HCN, with a dipole moment of 3.0 D, is only 9 cm^{-1} [35] and the dipole moment of **III** is even smaller than the experimental critical value of ca. 2.5 D required to observe a dipole-bound anion.[52]

Therefore, we present detailed results for the iminoammonium (HNNH$_3$) tautomer only. The relevant rotational energy level spacings for this tautomer are much smaller than the calculated values of E_{bind}. Hence, non-BO coupling between the electronic and rotational degrees of freedom is expected to be of secondary importance for this anion and is not considered in this study.

3.1. MP2 Geometries and Harmonic Frequencies. The C_s symmetry local minima on the MP2 potential energy surface of the neutral and anionic molecule are characterized in Table 1. We studied the dependence of the dipole moment of the neutral molecule on geometrical displacements induced by electron attachment. In Table 1 we report the values of the neutral's dipole moment calculated using the SCF and QCISD densities at the neutral and at the anion geometries. (QCISD is an approximation to the CCSD method.[55])

Our calculations indicate that the geometries of the neutral and anion differ only slightly; see Table 1. In particular, electron attachment leads to elongation of all bonds by 0.001 Å, and the valence as well as dihedral angles change by less than 1.2°. These small geometrical distortions cause an increase of the dipole moment, μ, of the neutral by 0.03 D at the SCF level, and 0.02 D at the QCISD level. These changes are very similar to those reported recently for HPPH$_3$,[26] and much smaller than for hydrogen-bonded systems, which we have studied previously,[33−36] and reflect the fact that the bonding in the neutral HNNH$_3$ is rigid, as it is in the case of HPPH$_3$.

The barrier to rotation around the N−N bond is 601 cm^{-1} (1.72 kcal/mol) for the neutral and 539 cm^{-1} (1.54 kcal/mol) for the anion. We verified that the anion remains electronically stable in the course of rotation around the N−N bond.
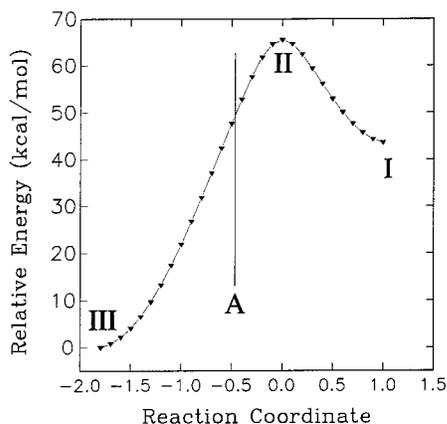
Figure 3. The minimum energy reaction path for the unimolecular tautomerization HNNH$_3$ $\leftrightarrow$ H$_2$NNH$_2$ of the neutral system. The path for the anion is very similar and lies close to this reported for the neutral molecule. The vertical line (A) indicates the border of electronic stability for the anionic system (the anion remains stable only to the right of this line).

The (unscaled) harmonic MP2 frequencies for the local minima are also reported in Table 1. The frequencies of the stiff stretching modes usually decrease upon electron attachment, and the largest shift of 20 cm^{-1} is for the eighth a' mode. On the contrary, the frequencies of the soft modes usually increase upon electron attachment and the largest shift of 23 cm^{-1} occurs for the first a' mode. Due to a partial cancelation of the frequency shifts, the change of the total zero-point vibrational energy upon electron attachment is rather small and amounts to -20 cm^{-1}.

We also investigated the pathway for unimolecular tautomerization of the anion and the neutral systems; see Figure 3. We located transition states on the neutral and anionic potential energy surfaces, and we give their geometrical parameters in Table 2. The unscaled harmonic MP2 frequencies as well as the neutral dipole moment for both geometries are also reported. Tautomerization of the neutral proceeds from the HNNH$_3$ species by migration of the atom labeled H$_3$ in Figure 1 toward N$_2$. At the transition state, which lies 23.58 kcal/mol above HNNH$_3$, H$_3$ resides between N$_1$ and N$_2$ and the N$_2$$-H_6$ bond has moved to the right, thus producing a transition state with no symmetry planes or axes (i.e., belonging to the C_1 point

group). Further along the reaction path, H$_3$ moves closer to N$_2$ and forms the N$_2$$-H_3$ bond as the N$_1$$-H_3$ bond is broken. Finally, along the reaction path, to reduce repulsion between the two nitrogen-centered lone pairs that thus arise in the H$_2$NNH$_2$ product, a small rotation then occurs about the N$_1$$-N_2$ bond, allowing the product to assume the gauche conformation shown as **III** in Figure 1. In the case of the reaction path for tautomerization of the anion, beginning at the (HNNH$_3$)$^-$ structure (described in detail in Table 2), this path reaches a transition state lying 25.58 kcal/mol higher. At all points along this portion of the path, the anion is electronically stable with respect to the neutral species. However, as the transition state is passed and the reaction path is followed onward toward the (H$_2$NNH$_2$)$^-$ product, a point is reached ca. 9 kcal/mol below the transition state (see the vertical line marked as A in Figure 3) at which the anion becomes electronically unstable (i.e., beyond which autodetachment will occur).

We also calculated the Franck$-$Condon (FC) factors for ((HNNH$_3$)$^-$/HNNH$_3$) using the MP2 geometrical Hessians and equilibrium geometries.[60,61] The intensity for the 0$-$0 transition was normalized to one, and all other intensities were scaled accordingly. The position of the 0$-$0 transition of 1095 cm^{-1}, which is equivalent to the adiabatic electron affinity of HNNH$_3$, was determined from the difference in the CCSD(T) energies of HNNH$_3$ and (HNNH$_3$)$^-$ at their respective MP2 minimum geometries (1075 cm^{-1}) and corrected for the difference in the zero-point vibrational energies (20 cm^{-1}) determined at the MP2 level. We found that there is no FC factor that exceeds 1% relative to the 0$-$0 transition (excluding the 0$-$0 FC factor). Thus we predict that the photodetachment spectrum of (HNNH$_3$)$^-$ should possess no vibrational structure beyond that of the 0$-$0 peak.

3.2. Electron Binding Energies. The anion is electronically bound not only in the neighborhood of the C_s minimum but also around the C_1 transition state; see Table 3. Taking into account the fact that the H$_2$NNH$_2$ tautomer cannot support an extra electron, we conclude that the anionic and neutral potential energy surfaces must cross in the region between the transition state and the equilibrium geometry of H$_2$NNH$_2$. It can therefore be concluded that the (HNNH$_3$)$^-$ anion, once formed, could exist for a long time.

The electron binding energy was partitioned into *incremental* contributions calculated at "successive" levels of theory (KT,

TABLE 2: Geometries and Harmonic Vibrational Frequencies for the Transition States on the Neutral and Dipole-Bound Anionic Surfaces for the Tautomerization HNNH$_3$ $\leftrightarrow$ H$_2$NNH$_2$^{a} (Frequencies in cm^{-1}, Distances (r) in Å, Valence (α) and Dihedral (δ) Angles in Degrees, Dipole Moment μ of the Neutral Dimer in D, Zero-Point Vibrational Energies (E_0^{vib}) in kcal/mol^b

| | | $\mu_{neutral}$ | | | |
system	geometry	SCF	QCISD	frequencies	E_0^{vib}
HNNH$_3$	r(N$_1$N$_2$) = 1.602, r(N$_1$H$_3$) = 1.101 r(N$_2$H$_3$) = 1.416, r(N$_1$H$_4$) = 1.016 r(N$_1$H$_5$) = 1.015, r(N$_2$H$_6$) = 1.032 α(N$_1$N$_2$H$_6$) = 100.65, α(N$_1$N$_2$H$_3$) = 42.23 α(N$_2$N$_1$H$_3$) = 59.81, α(N$_2$N$_1$H$_4$) = 115.30 α(N$_2$N$_1$H$_5$) = 108.43, δ(H$_3$N$_1$N$_2$H$_6$) = $-$104.56 δ(H$_5$N$_1$N$_2$H$_6$) = 137.09, δ(H$_4$N$_1$N$_2$H$_6$) = 7.81	3.59	3.71^c	ω_1 = 1609i, ω_2 = 285 ω_3 = 742, ω_4 = 919 ω_5 = 972, ω_6 = 1359 ω_7 = 1449, ω_8 = 1557 ω_9 = 2754, ω_{10} = 3430 ω_{11} = 3541, ω_{12} = 3676	29.57
HNNH$_3$$^-$	r(N$_1$N$_2$) = 1.600, r(N$_1$H$_3$) = 1.104 r(N$_2$H$_3$) = 1.409, r(N$_1$H$_4$) = 1.016 r(N$_1$H$_5$) = 1.015, r(N$_2$H$_6$) = 1.032 α(N$_1$N$_2$H$_6$) = 100.67, α(N$_1$N$_2$H$_3$) = 42.47 α(N$_2$N$_1$H$_3$) = 59.44, α(N$_2$N$_1$H$_4$) = 115.34 α(N$_2$N$_1$H$_5$) = 108.69, δ(H$_3$N$_1$N$_2$H$_6$) = $-$104.80 δ(H$_5$N$_1$N$_2$H$_6$) = 136.63, δ(H$_4$N$_1$N$_2$H$_6$) = 7.32	3.57	3.68^d	ω_1 = 1662i, ω_2 = 294 ω_3 = 748, ω_4 = 925 ω_5 = 975, ω_6 = 1359 ω_7 = 1444, ω_8 = 1556 ω_9 = 2734, ω_{10} = 3430 ω_{11} = 3535, ω_{12} = 3671	29.55

^{a} For the numbering of atoms, see Figure 1 (structure **II**). ^{b} MP2 results obtained with the aug-cc-pVDZ basis set supplemented with the 6s6p4d diffuse set. ^{c} MP2, MP3, and MP4(SDQ) values of dipole moment: 3.85, 3.76, and 3.74 D, respectively. ^{d} MP2, MP3, and MP4(SDQ) values of dipole moment: 3.82, 3.73, and 3.71 D, respectively.

TABLE 3: Incremental Electron Binding Energies^a (cm^{-1}) for the Anionic State of HNNH₃

component	(HNNH₃)$^-$ $C_s{}^b$	(HNNH₃)$^-$ $C_s{}^c$	transition state for (HNNH₃)$^-$, $C_1{}^d$
E_{bind}^{KT}	366	377	21
$\Delta E_{bind}^{SCF-ind}$	49	51	1
$\Delta E_{bind}^{MP2-disp}$	370	382	31
$\Delta E_{bind}^{MP2-no-disp}$	−21	−23	14
ΔE_{bind}^{MP3}	−22	−22	−7
ΔE_{bind}^{MP4}	72	73	11
$\Delta E_{bind}^{CCSD(T)}$	235	238	127
sum	1049	1076	198

^{a} Results obtained with the aug-cc-pVDZ basis set supplemented with the 6s6p4d diffuse set. ^{b} For the geometry of the neutral. ^{c} For the geometry of the anion. ^{d} For the geometry of the anion.

SCF, MPn ($n = 2, 3, 4$), and CCSD(T)), and the results for the optimal C_s structures of the neutral and the anion are presented in the second and third columns of Table 3. In the KT approximation, the electron binding energy results from the electrostatic and exchange interactions of the extra electron with the SCF charge distribution of the neutral molecule (primarily characterized by the dipole moment, but interactions with higher permanent multipoles and penetration effects are also included). The value of E_{bind}^{KT} increases by 11 cm^{-1} upon geometry relaxation from the neutral to the anionic structure, which is consistent with the small increase in dipole moment accompanying this geometry change (see Table 1).

The SCF binding energies include orbital relaxation and thus take into account static polarization of the neutral molecule by the extra electron and the secondary effect of back-polarization. The 49−51 cm^{-1} values of the orbital relaxation *correction* to E_{bind}^{KT}, denoted $\Delta E_{bind}^{SCF-ind}$ in Table 3, are not negligible and represent about 5% of the total E_{bind}.

The contribution denoted $\Delta E_{bind}^{MP2-disp}$ results from dynamical correlation between the extra electron and the electrons of the neutral molecule. This stabilizing effect, caused by quantum mechanical charge fluctuations, is similar in magnitude to E_{bind}^{KT}, see Table 3. This finding is consistent with our earlier results for other dipole-bound anions[26,31−37] and has important implications for designing model potentials to describe dipole-bound anions and solvated electrons.[62,63] The value of $\Delta E_{bind}^{MP2-disp}$ increases from 370 cm^{-1} at the optimal geometry of the neutral to 382 cm^{-1} at the optimal geometry of the anion.

In addition to the dispersion interaction, electron correlation may also affect the charge distribution (and dipole moment) of the neutral molecule and thus its electrostatic interaction with the extra electron. This effect first appears at the MP2 level and is denoted by $\Delta E_{bind}^{MP2-no-disp}$. In the case of HNNH₃, the

MP2 electron correlation effects reduce the dipole moment of the neutral system by only 0.01 D in comparison with the SCF value (see Table 1) and higher order corrections are also very small. Therefore, the values of $\Delta E_{bind}^{MP2-no-disp}$ are small for this system.

As Table 3 shows, the convergence of the MP series for the electron binding energy in HNNH₃$^-$ is slow. The contribution from ΔE_{bind}^{MP3} is not negligible and is destabilizing. The contribution from ΔE_{bind}^{MP4} represents ca. 7% of E_{bind}, and higher-order electron correlation effects, approximated here by $\Delta E_{bind}^{CCSD(T)}$ (the *difference* in the CCSD(T) and MP4 binding energies), are significant, stabilizing, and responsible for 22% of the net electron binding energy. They produce our final prediction for the vertical electron detachemnt energy of 1076 cm^{-1} for P₂H₄$^-$.

At the C_1 transiton state of the anion the dipole moment of the neutral is 3.7 D and the electron binding energy is 22, 67, and 198 cm^{-1} at the SCF, MP2, and CCSD(T) levels, respectively; see the fourth column of Table 3. Thus electron correlation effects represent 89% of the electron binding energy at the transition state. This contribution is comparable to that for the minimum energy structure of HPPH₃$^-$, for which the dipole moment of the neutral was also found to be 3.7 D.[26] Another interesting feature of the anionic transition state is that the $\Delta E_{bind}^{MP2-no-disp}$ term is stabilizing, which is consistent with the fact that electron correlation effects increase the dipole moment of the neutral; see Table 2.

The contributions to ΔE_{bind}^{MP4} and $\Delta E_{bind}^{CCSD(T)}$ from various classes of excitations are collected in Table 4 and will now be discussed for the anionic minimum geometry. The MP4 contribution from double and quadruple excitations, $\Delta E_{bind}^{MP4(DQ)}$ is destabilizing and amounts to −9 cm^{-1}. The contributions from single excitations, given by the difference between $\Delta E_{bind}^{MP4(SDQ)}$ and $\Delta E_{bind}^{MP4(DQ)}$, is stabilizing and equal to 43 cm^{-1}. The contribution from triple excitations, given by the difference between $\Delta E_{bind}^{MP4(SDTQ)}$ and $\Delta E_{bind}^{MP4(SDQ)}$, is also stabilizing and of the same importance (39 cm^{-1}). The final fourth-order contribution $\Delta E_{bind}^{MP4(SDTQ)}$ amounts to 73 cm^{-1}.

The effect of single excitations is 5 times more important when evaluated in the framework of coupled-cluster theory where its contribution, calculated as the difference between E_{bind}^{CCSD} and E_{bind}^{CCD}, amounts to 236 cm^{-1}. The contribution from noniterative triple excitations, calculated as the difference between $E_{bind}^{CCSD(T)}$ and E_{bind}^{CCSD}, contains the fourth-order contribution with the CCSD amplitudes and a fifth-order term,[55] which are labeled T4(CCSD) and T5(CCSD), respectively, in Table 4. The fourth-order contribution with the CCSD amplitudes is highly stabilizing and amounts to 113 cm^{-1}, while the fifth-order contibution is slightly destabilizing and amounts to −25 cm^{-1}. Hence, the contribution from noniterative triple excitations

TABLE 4: Contributions of Various Classes of Excitations to E_{bind} (cm^{-1}) at the Neutral and Anionic Equilibrium Geometries from Tables 1 and 2^a

method	(HNNH₃)$^-$ $C_s{}^b$ E_{bind}	(HNNH₃)$^-$ $C_s{}^b$ ΔE_{bind}	(HNNH₃)$^-$ $C_s{}^c$ E_{bind}	(HNNH₃)$^-$ $C_s{}^c$ ΔE_{bind}	transition state for (HNNH₃)$^-$, $C_1{}^d$ E_{bind}	transition state for (HNNH₃)$^-$, $C_1{}^d$ ΔE_{bind}
UMP4(DQ)	734	−8	756	−9	60	−1
UMP4(SDQ)	776	33	799	34	65	5
UMP4(SDTQ)	814	72	838	73	71	11
CCD	730	−4	752	−4	59	−1
CCSD	962	187	988	189	152	87
CCSD(T)	1049	235	1076	238	198	127
T4(CCSD)		111		113		56
T5(CCSD)		−24		−25		−10

^{a} Results obtained with the aug-cc-pVDZ basis set supplemented with the 6s6p4d diffuse set. ^{b} For the geometry of the neutral. ^{c} For the geometry of the anion. ^{d} For the geometry of the anion.

is stabilizing, amounts to 88 cm^{-1}, and is dominated by the fourth-order contribution (with the CCSD amplitudes).

Higher than fourth-order electron correlation contributions to E_{bind} may also be extracted from the data collected in Table 4. The difference between E_{bind}^{CCD} and $E_{bind}^{MP4(DQ)}$ is very small and amounts to -5 cm^{-1}. However, when single excitations are included, the situation is quite different; indeed, the difference between E_{bind}^{CCSD} and $E_{bind}^{MP4(SDQ)}$ amounts to 189 cm^{-1}. These results support our earlier conclusions that the MP4 treatment of electron correlation effects is not sufficient for dipole-bound anions.[26,31-36] The contribution from triple excitations proved to be very sensitive to the form of amplitudes of the single and double excitations. For this dipole-bound anion it may be necessary to adopt methods such as CCSDT-1 or CCSDT, which treat high-order correlation effects more accurately than does the CCSD(T) method.[55]

4. Conclusions

Our results indicate that the HNNH$_3$ tautomer of hydrazine can bind an electron by 1076 cm^{-1}, whereas the well-known H$_2$NNH$_2$ tautomer cannot. This suggests a practical route to formation of the HNNH$_3$ tautomer through photodetachment of the excess electron from N$_2$H$_4^-$. The neutral and anionic HNNH$_3$ are predicted to be kinetically stable with respect to tautomerization (having barriers of 23.6 and 25.6 kcal/mol, respectively), though thermodynamically unstable by 43.6 and 40.5 kcal/mol (with respect to the neutral H$_2$NNH$_2$), respectively.

The excess electron in (HNNH$_3$)$^-$ is already bound due to the dipole potential of the neutral as obtained at the KT level of theory, but electron correlation effects contribute 60% to the total value of the electron binding energy at the highest CCSD(T) level of theory employed here, even though the dipole moment of the neutral is *decreased* by 1.3% when electron correlation effects are included.

The second-order dispersion stabilization was found to be the most important for the stabilization of the excess electron, as it is responsible for 35% of the total electron binding energy. The contributions to E_{bind} from single and triple excitations proved to be more significant in the CCSD(T) than in the MP4 approach.

The electronic stability of the iminoammonium anion is more than 3 times larger than that found previously for its phosphorus analogue ((HPPH$_3$)$^-$),[26] as dictated by the significant difference in dipole moments of the neutral species (3.7 D for HPPH$_3$ vs 5.4 D for HNNH$_3$).

References and Notes

(1) Wagman, D. D.; Evans, W. H.; Parker, V. B.; Schumm, R. H.; Halow, I.; Bailey, S. M.; Churney, K. L.; Nuttall, R. L. The NBS Tables of Chemical Thermodynamics Properties. *J. Phys. Chem. Ref. Data* **1982**, Suppl. 2, 11.

(2) Vaghjiani, G. L. *J. Phys. Chem. A* **1997**, *101*, 4167.

(3) Vaghjiani, G. L. *J. Phys. Chem.* **1993**, *98*, 2123.

(4) Kohata, K.; Fukuyama, T.; Kuchitsu, K. *J. Phys. Chem.* **1982**, *86*, 602.

(5) Beihl, H.; Stuhl, F. *J. Photochem. Photobiol. A: Chem.* **1991**, *59*, 135.

(6) Lindberg, P.; Raybone, D.; Salthouse, J. A.; Watkinson, T. M.; Whitehead, J. C. *Mol. Phys.* **1987**, *62*, 1297.

(7) Vinogradov, I. P.; Firsov, V. V. *Opt. Spectrosc. USSR* **1982**, *53*, 26.

(8) Diesen, R. W. *J. Chem. Phys.* **1963**, *39*, 2121.

(9) Filseth, S. V.; Danon, J.; Feldmann, D.; Campbell, J. D.; Welge, K. H. *Chem. Phys. Lett.* **1979**, *63*, 615.

(10) Hack, W.; Rathmann, K. *Z. Phys. Chem. (Munich)* **1992**, *176*, 151.

(11) Fink, W.; Pan, D. C.; Allen, L. C. *J. Chem. Phys.* **1967**, *47*, 895.

(12) Mosquera, R. A.; Vasquez, S.; Rios, M. A.; Van Alsenoy, C. *J. Mol. Struct.* **1990**, *206*, 4.

(13) Jarvie, J. O.; Rauk, A. *Can. J. Chem.* **1974** *52*, 2785.

(14) Riggs, N.; Radom, L. *Aust. J. Chem.* **1986**, *39*, 1917.

(15) DeFrees, D. J.; Raghavachari, K.; Schlegel, H. B.; Pople, J. A. *J. Am. Chem. Soc.* **1982**, *104*, 5576.

(16) Rao, B. G.; Singh, U. C. *J. Am. Chem. Soc.* **1991**, *113*, 4381.

(17) Schlegel, H. B.; Skancke, A. *J. Am. Chem. Soc.* **1993**, *115*, 7465.

(18) Habas, M.-P.; Baraille, I.; Larrieu, C.; Chaillet, M. *Chem. Phys.* **1997**, *219*, 63.

(19) Schmitz, B. K.; Euler, W. B. *J. Mol. Struct. (THEOCHEM)* **1992**, *257*, 227.

(20) Chung-Phillips, A.; Jebber, K. A. *J. Chem. Phys.* **1995**, *102*, 7080.

(21) Pople, J. A.; Raghavachari, K.; Frisch, M. J.; Binkley, J. S.; Schleyer, P.v. R. *J. Am. Chem. Soc.* **1983**, *105*, 6389.

(22) Ding, F.-J.; Zhang, L.-F. *Int. J. Quantum Chem.* **1997**, *64*, 447.

(23) Pople, J. A.; Curtiss, L. A. *J. Chem. Phys.* **1991**, *95*, 4385.

(24) Yalcin, T.; Suzer, S. *J. Mol. Struct.* **1992**, *266*, 353.

(25) Simons, J.; Jordan, K. D. *Chem. Rev.* **1987**, *87*, 535.

(26) Skurski, P.; Gutowski, M.; Simons, J. *J. Chem. Phys.*, in press.

(27) Jordan, K. D. *Acc. Chem. Res.* **1979**, *12*, 36.

(28) Jordan, K. D.; Luken, W. *J. Chem. Phys.* **1976**, *64*, 2760.

(29) Gutsev, G. L.; Sobolewski, A. L.; Adamowicz, L. *Chem. Phys.* **1995**, *196*, 1.

(30) Gutsev, G. L.; Adamowicz, L. *J. Phys. Chem.* **1995**, *99*, 13412.

(31) Gutowski, M.; Skurski, P.; Boldyrev, A. I.; Simons, J.; Jordan, K. D. *Phys. Rev. A* **1996**, *54*, 1906.

(32) Gutowski, M.; Skurski, P.; Simons, J.; Jordan, K. D. *Int. J. Quantum Chem.* **1997**, *64*, 183.

(33) Gutowski, M.; Skurski, P. *J. Chem. Phys.* **1997**, *107*, 2968.

(34) Gutowski, M.; Skurski, P. *J. Phys. Chem. B* **1997**, *101*, 9143.

(35) Gutowski, M.; Jordan, K. D.; Skurski, P. *J. Phys. Chem. A* **1998**, *102*, 2624.

(36) Skurski, P.; Gutowski, M. *J. Chem. Phys.* **1998**, *108*, 6303.

(37) Gutowski, M.; Skurski, P. Manuscript in preparation.

(38) Yokoyama, K.; Leach, G. W.; Kim, J. B.; Lineberger, W. C.; Boldyrev, A. I.; Gutowski, M. *J. Chem. Phys.* **1996**, *105*, 10706.

(39) Ramaekers, R.; Smith, D. M. A.; Smets, J.; Adamowicz, L. *J. Chem. Phys.* **1997**, *107*, 9475.

(40) Smith, D. M. A.; Smets, J.; Elkadi, Y.; Adamowicz, L. *J. Chem. Phys.* **1997**, *107*, 5788.

(41) Smith, D. M. A.; Smets, J.; Elkadi, Y.; Adamowicz, L. *J. Chem. Phys.* **1998**, *109*, 1238.

(42) Gutsev, G. L.; Bartlett, R. J. *J. Chem. Phys.* **1996**, *105*, 8785.

(43) Desfrançois, C.; Abdoul-Carime, H.; Khelifa, N.; Schermann, J. P. *Phys. Rev. Lett.* **1994**, *73*, 2436.

(44) Stockdale, J. A.; Davis, F. J.; Compton, R. N.; Klots, C. E. *J. Chem. Phys.* **1974**, *60*, 4279.

(45) Hasemi, R.; Illenberger, E. *J. Phys. Chem.* **1991**, *95*, 6402.

(46) Bailey, C. G.; Dessent, C. E. H.; Johnson, M. A.; Bowen, K. H., Jr. *J. Chem. Phys.* **1996**, *104*, 6976.

(47) Castleman, A. W., Jr.; Bowen, K. H., Jr. *J. Phys. Chem.* **1996**, *100*, 12911.

(48) Fermi, E.; Teller, E. *Phys. Rev.* **1947**, *72*, 399.

(49) Wightman, A. S. *Phys. Rev.* **1950**, *77*, 521.

(50) Levy-Leblond, J. M. *Phys. Rev.* **1967**, *153*, 1.

(51) Mittleman, M. H.; Myerscough, V. P. *Phys. Lett.* **1966**, *23*, 545.

(52) Crawford, O. H. *Mol. Phys.* **1971**, *20*, 585.

(53) Garrett, W. R. *J. Chem. Phys.* **1982**, *77*, 3666.

(54) Koopmans, T. *Physica* **1934**, *1*, 104.

(55) Bartlett, R. J.; Stanton, J. F. In *Reviews in Computational Chemistry*; Lipkowitz, K. B., Boyd, D. B., Eds.; VCH Publishers, Inc.: New York, 1994; Vol. V.

(56) Taylor, P. R. In *Lecture Notes in Quantum Chemistry II*; Roos, B. O., Ed.; Springer-Verlag: Berlin, 1994.

(57) Kendall, R. A.; Dunning, T. H., Jr.; Harrison, R. J. *J. Chem. Phys.* **1992**, *96*, 6796.

(58) Gutowski, M.; Simons, J. *J. Chem. Phys.* **1990**, *93*, 3874.

(59) Frisch, M. J.; Trucks, G. W.; Schlegel, H. B.; Gill, P. M. W.; Johnson, B. G.; Robb, M. A.; Cheeseman, J. R.; Keith, T.; Petersson, G. A.; Montgomery, J. A.; Raghavachari, K.; Al-Laham, M. A.; Zakrzewski, V. G.; Ortiz, J. V.; Foresman, J. B.; Cioslowski, J.; Stefanov, B. B.; Nanayakkara, A.; Challacombe, M.; Peng, C. Y.; Ayala, P. Y.; Chen, W.; Wong, M. W.; Andres, J. L.; Replogle, E. S.; Gomperts, R.; Martin, R. L.; Fox, D. J.; Binkley, J. S.; Defrees, D. J.; Baker, J.; Stewart, J. P.; Head-Gordon, M.; Gonzalez, C.; Pople, J. A. Gaussian 94, Revision B.1; Gaussian, Inc.: Pittsburgh, PA, 1995.

(60) Doktorov, E. V.; Malkin, I. A.; Man'ko, V. I. *J. Mol. Spectrosc.* **1977**, *64*, 302; **1975**, *56*, 1.

(61) Yang, D.-S.; Zgierski, M. Z.; Rayner, D. M.; Hackett, P. A.; Martinez, A.; Salahub, D. R.; Roy, P.-N.; Carrington, T., Jr. *J. Chem. Phys.* **1995**, *103*, 5335.

(62) Desfrançois, C. *Phys. Rev. A* **1995**, *51*, 3667.

(63) Barnett, R. N.; Landman, U.; Dhar, S.; Kestner, N. R.; Jortner, J.; Nitzan, A. *J. Chem. Phys.* **1989**, *91*, 7797.